

Changes in Ice Dendrite Size during Freezing Process in Gelatin Matrix as a Model Food System

Sang-Gi Min, Geun-Pyo Hong, Mi-Jung Choi^{1*}

Laboratory of Food Engineering, Department of Food Science and Biotechnology of Animal Resources,
College of Animal Husbandry, Konkuk University, Seoul 143-701, Korea

¹National Nanotechnology Center, National Science and Technology Development Agency, Pathumthani 12120, Thailand

모델 식품으로 젤라틴 매트릭스에서 동결과정에 따른 얼음 결정체 변화

민상기 · 홍근표 · 최미정^{1*}

건국대학교 축산식품생물공학전공, ¹태국 국립나노연구센터

Abstract

The objective of this study was to investigate the changes in ice dendrite size during freezing process in gelatin matrix as a model food system in order to provide mathematical relation between freezing condition and ice dendrite size. Gelatin gel as a model matrix was frozen in unidirectional Neumann's type of heat transfer. The thermograms' analysis allowed to determine the freezing temperature of the sample, the position of the freezing front versus time, and thus, freezing front rate. The morphology of ice dendrites was observed by scanning electron microscopy after freeze-drying. We observed that the means size of ice dendrite increased with the distance to the cooling plate; however, it decreased with the cooling rate and the cooling temperature. In addition, the shorter durations of the freeze-drying process was shorter decreasing the decreased the freezing front rate, resulted in their resulting in a larger pore size of the ice dendrite pores for the sublimation channel of that operate as water vapor sublimation channels. From these results, we could derive a linear regression as an empirical mathematical model equation between the ice dendrite size and the inverse of freezing front rate.

Key words : gelatin matrix, freezing, ice crystal size, freeze-drying, heat transfer

Introduction

In the field of food industry, the freezing process has various advantages that prolong the shelf-life, minimize the physico-chemical denaturalization, and prevent contamination of microorganism (Reid, 1990). These treatments can restrain the proliferation of microorganism in consequence of the diminution of water activity for the microorganism. However, it entails inevitably the formation of ice crystal by phase transformation of water, which is a main target in the freezing step. The structure and shape of ice crystal as well

as their ice dendrite size in the frozen food have a great effect on the rheological properties of food products and the processing characteristics (Bevilacqua *et al.*, 1979; Bomben *et al.*, 1982; Miyawaki *et al.*, 1992; Tamon *et al.*, 2001; Choi *et al.*, 2004)

Consequently, textural quality of frozen foods is strongly related to freezing process conditions which affect the formation of ice crystal size. In general, the size of ice crystal within food changes their mechanical and chemical structure. Many researchers have reported that in case of slow freezing rate for cells, the ice crystal begins to form from the extracellular, and then their growth of ice dendrites lead to be mechanically damaged (Cho, 1994). On the contrary, the fast freezing rate provokes a formation of small ice crystal in the extra- and intracellular cells, resulting in less damage of cell survival (Miyawaki *et al.*, 1992; Bevilacqua *et al.*,

*Corresponding author : Mi-Jung Choi, National Nanotechnology Center, National Science and Technology Development Agency, Pathumthani 12120, Thailand. Tel: 66-2564-7100; Fax: 66-2564-6981, E-mail: mijung@nanotec.or.th

1979). Experimentally, it is well known that fast freezing gives small and numerous crystals, whereas a slow freezing gives large and less numerous ice crystals. Therefore, controlling of freezing conditions (e.g., initial temperature, freezing rate, and etc) remains as major challenge in reaching the convenient and the conservative nutrition in the frozen food.

The selected gelatin as a model system is a high mass molecular hydrophilic protein obtained from by hydrolysis of insoluble water collagen. It can be mainly gained from the animal skin or bones such as beef and pork. Gelatin is primarily used as a gelling agent (Cho, 1994) forming transparent elastic thermoreversible gels on cooling approximately below 35°C, which dissolves at low temperature to give 'melt in the mouth' products with useful flavor-release. In addition, the amphiphilic nature of the molecules endows them with a useful emulsification (e.g. whipped cream) and foam-stabilizing properties (e.g. mallow foam). The other main advantage of the gelatin gel is its good transparency in an unfrozen state which allowed us to observe the crystallization phenomenon during the freezing stage (Cho, 1994).

Our experiments were carried out with gelatin gels in order to study microscopic structure and thermophysical properties. A freezing apparatus has been designed to ensure a step for temperature change for unidirectional heat transfer (Neumann's conditions). The ice crystal sizes were measured on the freeze-dried sample. Therefore, we analyzed the relation of ice crystal size depending on the process of the freezing step in the gelatin model systems, and then, with

these results, the change of the primary ice dendrite size was represented mathematically.

Materials and Methods

Sample Preparation

3% gelatin (Shinyo Pure Chemicals Co., Tokyo, Japan) solution was heated at 50°C until dissolved completely. This gelatin solution was then cooled down at the room temperature to obtain a gel form.

Freezing Apparatus

A freezing cell, similar to the one previously used by Woinet *et al.* (1998a), was thermally made of a 200 mm diameter acryl glass cylinder and a very thin flat bottom copper; the whole experimental device was designed to ensure one-dimensional heat transfer (Neumann's Model, Fig. 1) and a temperature changed step from the initial temperature to the cooling temperature. The sample exchanged heat principally with the copper plate, in one-dimensional heat transfer mode. Thermocouples were regularly placed at different levels (position of thermocouple from the bottom copper = 5, 10, 15, and 20 mm) on the symmetry axis of the freezing cell parallel to the isotherm planes. An acquisition device recorded the thermograms (Yokogawa, Japan).

Freezing and Freeze-drying Process

Frozen cylindrical samples were then freeze-dried in a lab-scale freeze-dryer (consisted of chamber, cold trap, vacuum

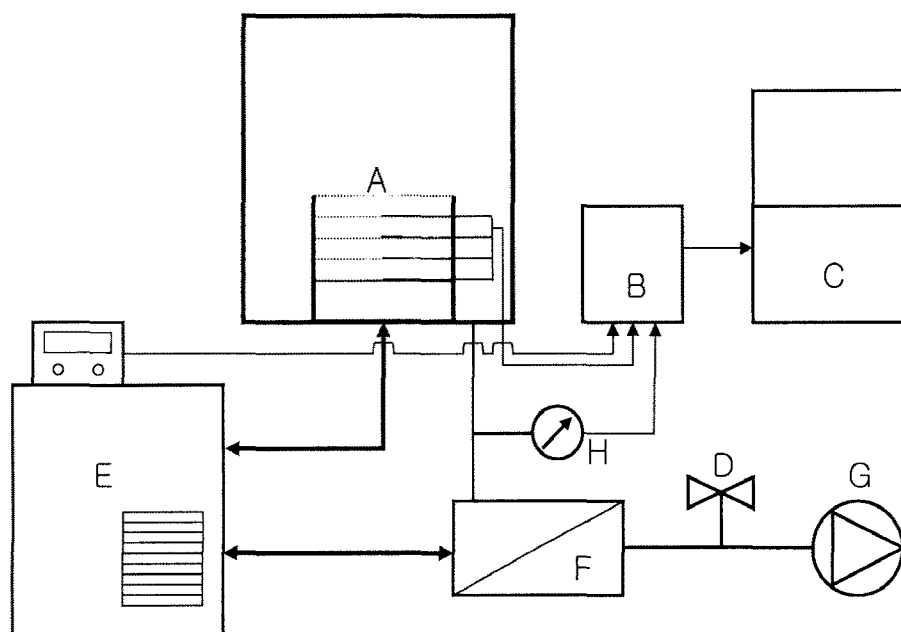


Fig. 1. Schematic diagram of the experimental apparatus for freezing and freeze-drying. A: freezing cell, B: data logger, C: acquisition device and computer, D: valve, E: cryostat and control unit, F: cold trap, G: vacuum pump, H: digital monometer.

pump, pressure gage, and digital monometer) at a maximum pressure of a 5 Pa (Fig. 1). The cold trap temperature was hold at -80°C and the pressure level was measured by digital manometer. Latent heat for sublimation was provided by radiation from the plates maintained at 25°C . The samples were frozen unidirectionally from the bottom at -30 , -24 , -18 and -12°C (cooling temperature, T_c), respectively and then freeze-dried under vacuum. During the freezing and freeze-drying process, the temperature profiles of gelatin matrix were measured. From these data, we calculate the freeze-drying time by the ending point of drying time when the sample temperature became increased and reached at constant temperature. When the freezing front reached the position of a thermocouple, it corresponded to a breakdown of the slope's value on the thermogram. Thus, from the database, the time at which the front reached each thermocouple was determined (Woinet *et al.*, 1998a).

Ice Dendrite Size and Morphology Analysis

Solid material after freeze drying was separated from the acryl-glass cylinder while maintaining its shape (Fig. 2). The freeze-dried samples were cut vertically at the half of each thermocouple height (2.5, 7.5, 12.5 or 17.5 mm) with a thin cutter. The freeze-dried samples were polished and sputter coated (E-1010, Hitachi, Japan) with a thin gold layer (13 mA, 93.3 Pa, 70 s). The samples were transferred under vacuum into a scanning electron microscope (Model S-3000N, Hitachi, Japan) where they were viewed and photographed. The size of ice crystals was characterized by determining the pore size left after freeze-drying the samples. The ice crystal, or in fact the pores, were measured by the means of the semi-automatic image analysis software (PPM, Arndt and Baumgartel GmbH, Bremen, Germany). The software was measured the size L , according to a corresponding previous calibration. For each slide, approximately 100 up to 300 crystals were measured, so giving the crystal size distribution.

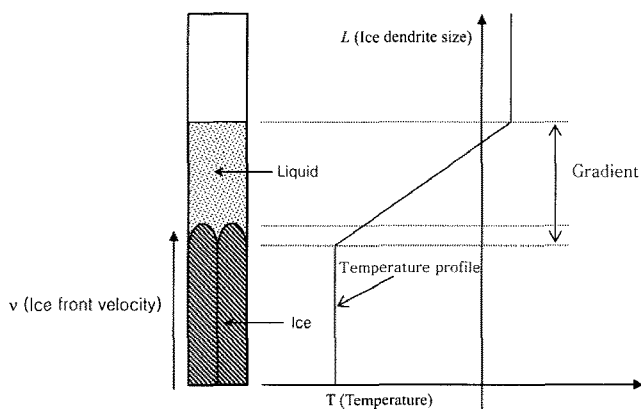


Fig. 2. Schematic diagram of directional solidification.

Results and Discussion

Freezing Front Rate and Time

The analysis of the thermogram recorded during the each freezing experiment gave us the exact freezing conditions, the position of the freezing front versus time, and the freezing front temperature. As pointed out previously, the freezing front location was determined from the thermograms' slope discontinuity. The freezing front temperature was the thermocouple temperature at the slope breakdown level.

The initial freezing front position was plotted at Fig. 3 on the time square root as a function of cooling temperature. All the results showed a linear relationship between the freezing front positions, noted s , and $t^{0.5}$ in agreement with the Neumann heat transfer model. Consequently, these plots could be interpreted by the following correlation:

$$s = a \times t^{0.5} + b \quad (1)$$

where a and b represents a freezing front rate constant as a slope and the intercept. This constant of slope decreased depending on increasing the freezing rate, where the cooling temperature decreased (Table 1) as previously observed by Woinet *et al.* (1998b). Therefore, it can be concluded that the overall freezing phenomenon was principally controlled by

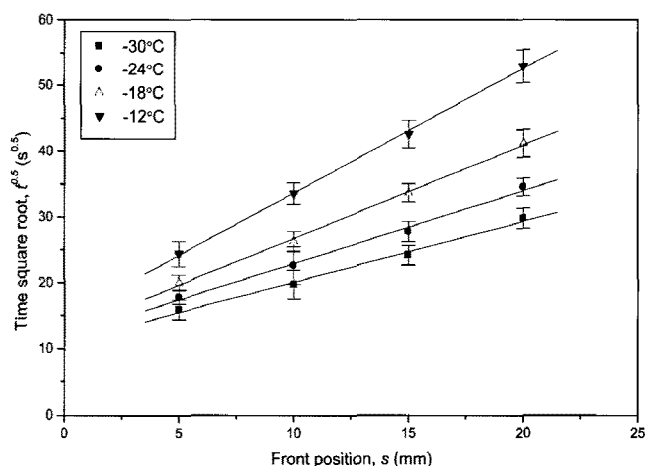


Fig. 3. Freezing time square ($t^{0.5}$) as a function of the front location (s) at different cooling temperatures.

Table 1. Parameters a and b of the relationship between freezing front time, $t^{0.5}$, and the distance, s , by linear regression such like, $s = a \times t^{0.5} + b$, a : slope, b : intercept, and R : correlation coefficient

Cooling temperature ($^{\circ}\text{C}$)	A	b	R
-30	0.9246	10.8401	0.9961
-24	1.1064	11.8669	0.9965
-18	1.4185	12.5657	0.9992
-12	1.8934	14.7251	0.9994

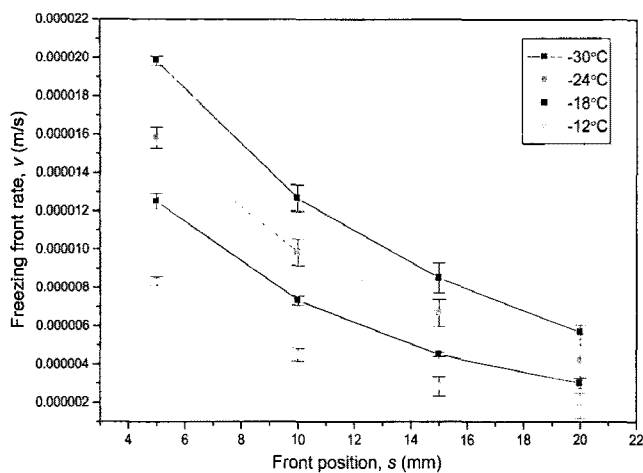


Fig. 4. Freezing front rate (v) as a function of the front location (s) at different cooling temperatures.

the freezing rate (heat transfer).

The freezing rate (n) was calculated from the temperature profile during freezing process as pointed out by Woinet *et al.* (1998). According to Fig. 4, the maximum freezing rate was calculated about 1.98×10^{-5} m/s on position 5 mm at $T_c = -30^\circ\text{C}$, and the minimum freezing rate was 0.83×10^{-6} m/s on position 20 mm at $T_c = -12^\circ\text{C}$ (Fig. 4). The cooling temperature was lower; the freezing front rate was higher in the same distance of thermocouple. Furthermore, depending on the distance from the bottom, the freezing front rate becomes faster at same cooling temperature. It could be supported by Woinet *et al.* (1998a; 1998b) that the freezing front rate is related to the temperature gradient in the frozen zone and to the front rate. Therefore, the gradient between the sample temperature and the cooling temperature during freezing process relies on the freezing time, that is, the rate of heat transfer and driving force of cooling temperature.

Thus, this freezing front rate, v , was calculated by derivation from the experimental curves $s = f(t)$ at different freezing front positions (Faydi *et al.*, 2001). As expected, we observed that for a given cooling temperature, the freezing front rate decreased with the distance to the cold wall, and secondly, for a given position, this freezing front rate increased when the cooling temperature decreased (Fig. 4).

Freeze-drying Time

In order to investigate the relationship between the cooling temperature T_c and the freeze-drying time t_{fd} , we represented mathematically the relation by linear regression (Fig. 5), such as

$$t_{fd} = a \cdot T_c + b \quad (2)$$

As shown in Fig. 5, the higher the cooling temperature, the shorter the freeze-drying time. Min (1994) and Kuprianoff

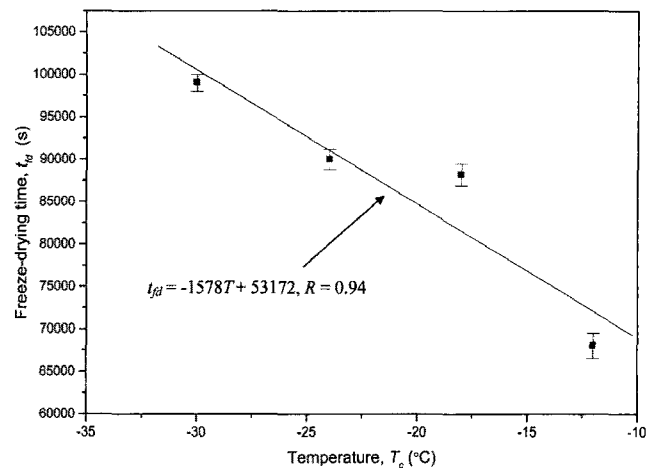


Fig. 5. Influence of cooling temperature on freeze-drying time in gelatin matrix.

(1962) have observed experimentally the same tendency as in our case, where the time of freeze-drying was longer according to the faster freezing rate in foodstuff. The freeze-drying time was for 27 hours at -30°C of cooling temperature. By contrast, it took 18 hours to finish the process of freeze drying at $T_c = -12^\circ\text{C}$. The fast freezing process requires more time for the sublimation during freeze-drying.

Our model system is a kind of unidirectional heat transfer system to form the ice crystal finger, which means that this ice channel is a route of transformation from the ice to the vapor during freeze-drying. So, the ice crystal size affects the resistance of sublimation of freeze-drying. In general, the small ice crystal is formed during fast freezing process.

It is empirically known that a quick freezing gives small crystals whereas a slow one gives larger crystals. Several authors (Kuprianoff, 1962; Bevilacqua *et al.*, 1979; Bomben and King, 1982) have proposed a simple relationship between the crystal size and the operating conditions, but no complete theoretical analysis has been yet developed.

Ice Dendrite Size Analysis

After cutting vertically the freeze dried sample, we measured the ice crystal size of the center of each position of thermocouple (2.5, 7.5, 12.5 and 17.5 mm).

Influence of cooling temperature

This parameter which determined the freezing front rate was varied between -30 and -12°C by using the cryostat, and all other parameters maintained constant. As presented in Figs. 6 and 7, the distribution of ice crystal size at $T_c = -30^\circ\text{C}$ was smaller and steeper slope than at $T_c = -12^\circ\text{C}$. These figures showed that there was a progressive enlargement of the ice crystal size when the freezing front rate (i.e., the cooling temperature) decreased. Martino *et al.* (1998) reported an

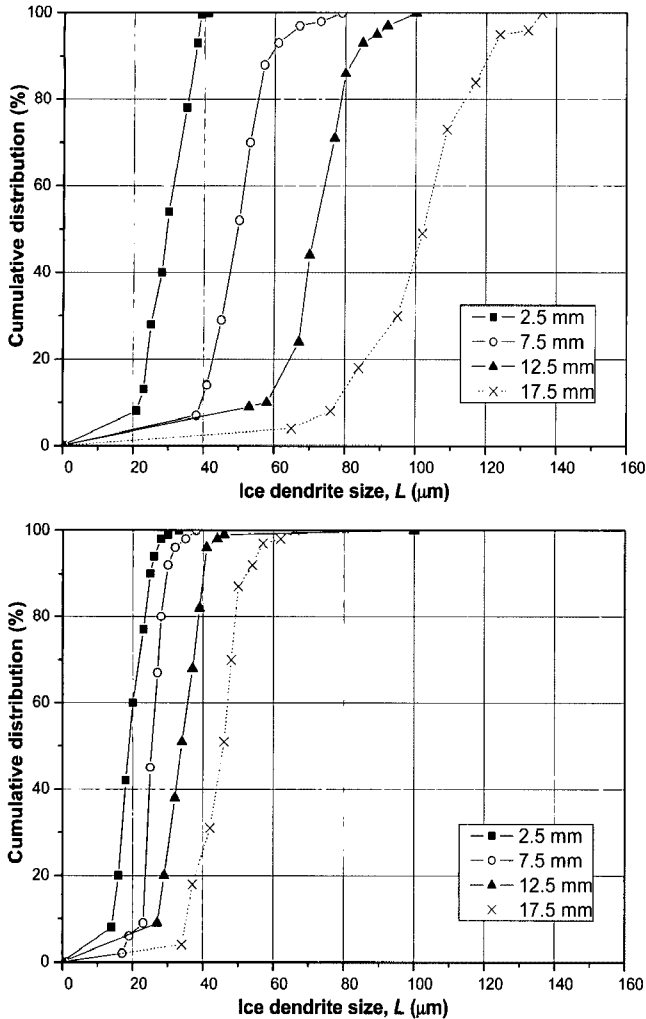


Fig. 6. Influence of the axial position at -12°C (upper) and -30°C (below) on evolution of ice crystal size.

increase of the mean ice crystal sizes regarding the influence of cooling parameters with beef when the cooling rate decreased.

Influence of axial position

The axial position of the thermocouple, corresponded to the distance to the cooling plate located at the bottom of the cooling cell. In a gelatin matrix, the maximum primary ice dendrite size was $99.94 \pm 17.21 \mu\text{m}$ at 17.5 mm and the minimum primary ice dendrite size was $30.55 \pm 4.88 \mu\text{m}$ at 2.5 mm from the experiment at $T_c = -12^\circ\text{C}$. The maximum primary ice dendrite size was $44.21 \pm 6.59 \mu\text{m}$ at 17.5 and the minimum primary ice dendrite size was $18.51 \pm 4.35 \mu\text{m}$ at 2.5 mm from the experiment at $T_c = -30^\circ\text{C}$.

The evolution of ice crystal size with the position in the gelatine matrix or with the square root of time (Eq. (1)) can be considered as linear fit. The Fig. 7 presented that the ice crystal size increased strongly with the distance from the cooling copper, i.e., when the freezing front rate decreased. Other authors studied the evolution of the crystalline size

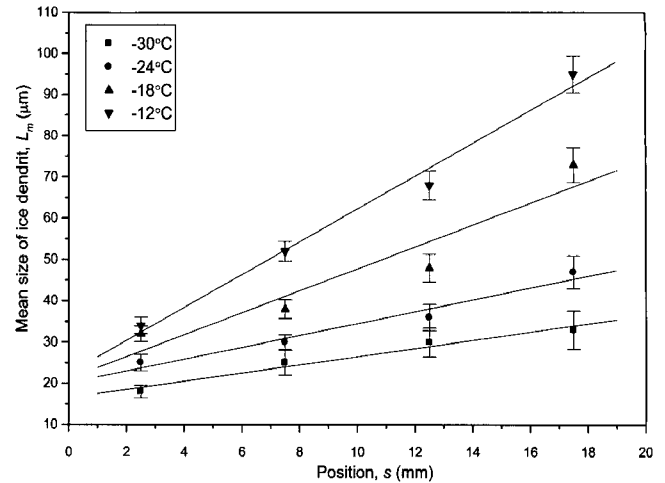


Fig. 7. Evolution of ice crystal mean size (L_m) depending on the axial position (s).

with different materials as a function of heat transfer parameters. Bomben *et al.* (1982) and Miyawaki *et al.* (1992) observed experimentally the same tendency as in our case with foodstuff and with equivalent crystal sizes. From the results, the ice crystal mean size L_m was calculated by linear regression in relation of the distance s. Table 2 showed these parameters as follows:

$$L_m = a \times s + b \tag{3}$$

Finally, the primary ice dendrite crystal size was fitted as a function of the inverse freezing front rate, $1/v$ of each position (Fig. 8). From the measurement of the ice dendrite mean size depending on the freezing rate, an empirical mathematical model could be provided as follows:

$$L_m = a \times 1/v + b \tag{4}$$

where, L_m = ice dendrite mean size, $1/v$ = freezing rate inverse, a and b = constants

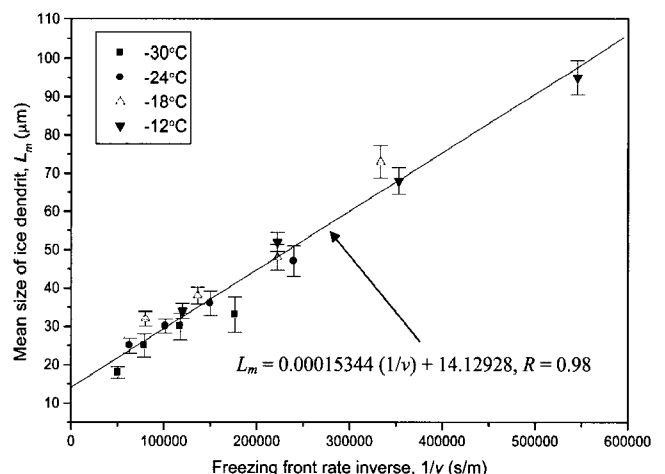


Fig. 8. Evolution of the ice dendrite mean size (L_m) as a function of the freezing front rate inverse ($1/v$) at different cooling temperature.

Table 2. Parameters of a (slope), b (intercept) and R from the linear regression relationship between ice dendrite mean size (L_m) and distance (s)

Cooling temperature (°C)	A	b	R
-30	1.00	16.50	0.9837
-24	1.44	20.10	0.9816
-18	2.66	21.15	0.9496
-12	3.98	22.45	0.9928

We obtained a linear regression between freezing front rate inverse $1/v$ and ice dendrite mean size, L_m . The ice dendrite size became smaller as the freezing rate increased, reversely when the freezing rate was slower; the primary ice dendrite size became larger.

Morphology Analysis

We observed the morphology of the ice crystal size and the structure of ice dendrite in gelatin depending on freezing rate by SEM. Figs. 9 and 10 showed that the ice dendrite size decreased as a function of the freezing rate at the same distance, besides at the same position, the ice crystal size increased at high cooling temperature. By the theory of Tamman, the quick freezing gave small and numerous crys-

tals whereas a slow freezing gave large and less numerous ice crystals (Bevilacqua and Zaritzky, 1982).

It was shown that freezing process effects the change of ice dendrite size during freezing process in gelatin matrix. The primary ice dendrite size became smaller as the freezing rate increased, reversely when the freezing rate was slower; the primary ice dendrite size became larger. Finally, we obtained a linear regression between freezing rate inverse $1/v$ and primary ice dendrite size, L_m shown by Eq. (4).

Acknowledgments

The authors wish to thank Mr. IN, Dae-Sik for his contributions.

References

1. Bevilacqua, A. and Zaritzky, N. E. (1982) Ice recrystallization in frozen beef. *J. Food Sci.* **47**, 892-899.
2. Bevilacqua, A., Zaritzky, N. E., and Calvelo, A. (1979) Histological measurement in frozen beef. *J. Food Technol.* **14**, 237-251.
3. Bomben, J. L. and King, C. J. (1982) Heat and mass transfer in the freezing of apple tissue. *J. Food Eng.* **17**, 615-632.
4. Cho, K. W. (1994) *Theory and Practice of frozen foods*;

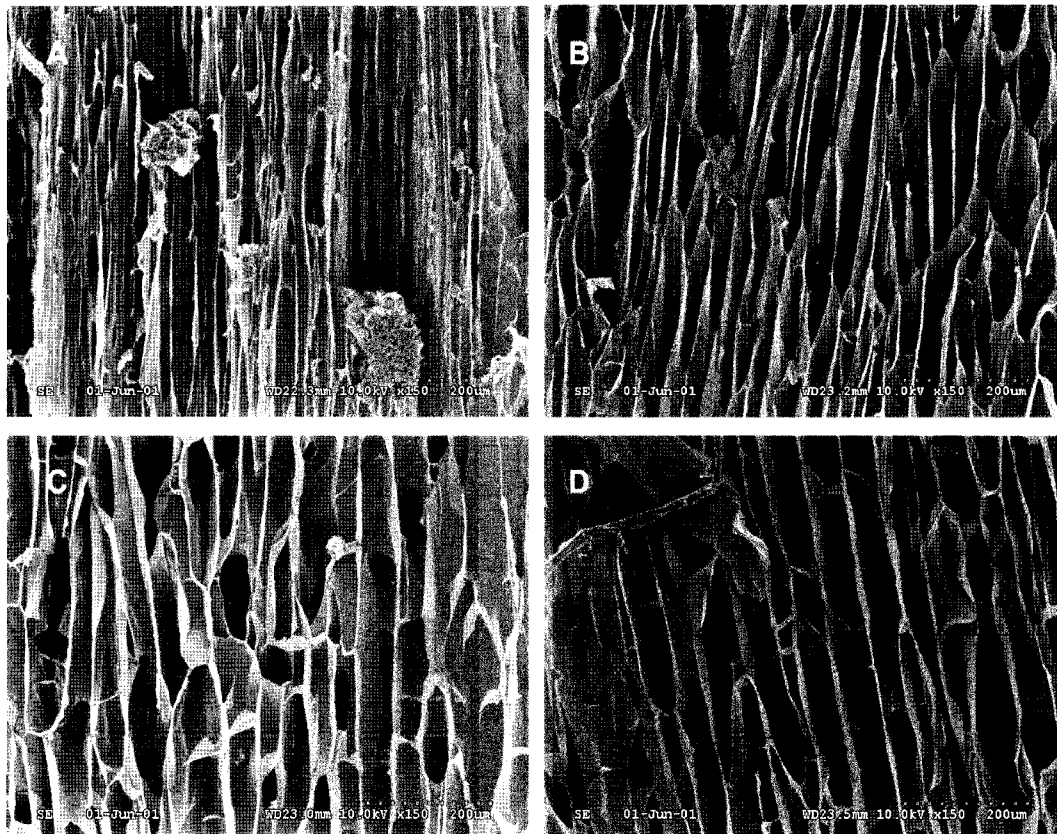


Fig. 9. Scanning electron microscopic image of ice dendrite in 4 different positions ($T_c = -18^\circ\text{C}$), A: 2.5 mm, B: 7.5 mm, C: 12.5 mm, and D: 17.5 mm.

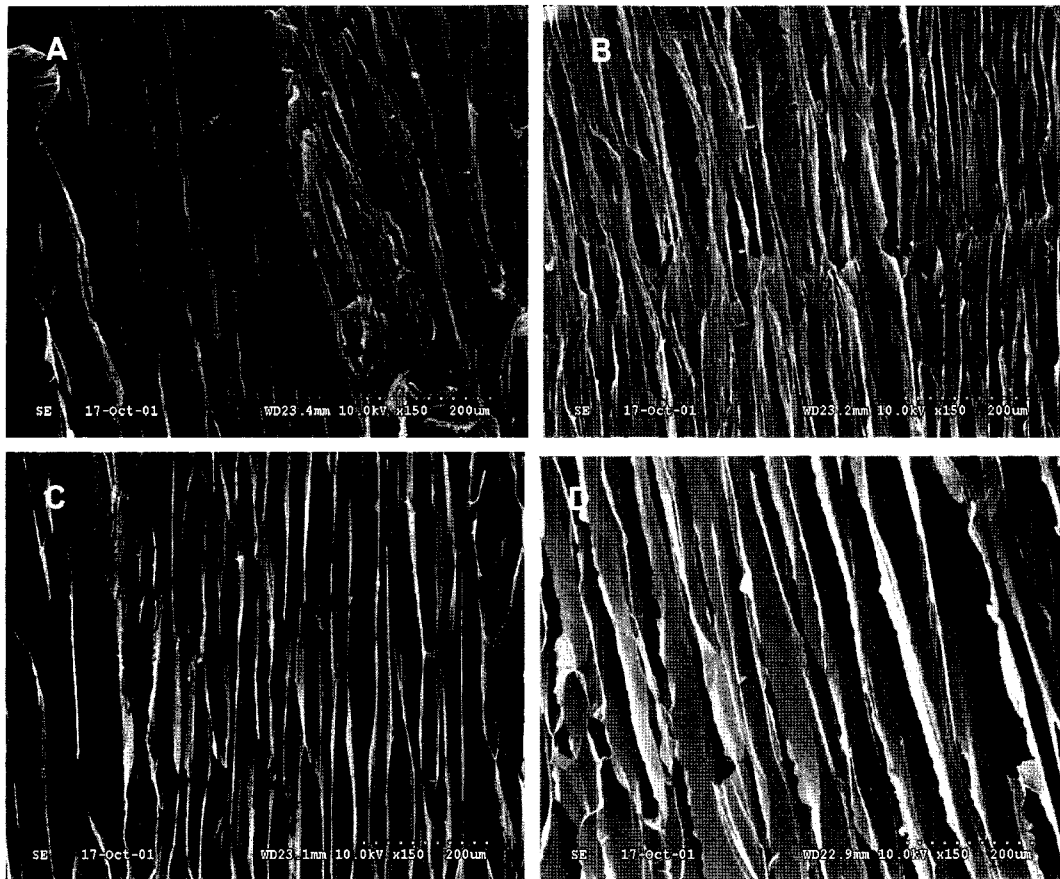


Fig. 10. Scanning electron microscopic image of ice dendrite in 4 different positions ($T_c = -30^\circ\text{C}$), A: 2.5 mm, B: 7.5 mm, C: 12.5 mm, and D: 17.5 mm.

Yoolim Press, Seoul.

5. Choi, M. J., Briançon, S., Andrieu, J., Min, S. G. and Fessi, H. (2004) Effect of freeze-drying process conditions on the stability of nanoparticles. *Drying Technol.* **22**, 335-346.
6. Faydi, E., Andrieu, J. and Laurent, P. (2001) Experimental study and modeling of the ice crystal morphology of model standard ice cream. Part I: Direct characterization method and experimental data. *J. Food Eng.* **48**, 283-291.
7. Kuprianoff, J. (1962) Some factors influencing the reversibility of freeze-drying of foodstuffs. In *Freeze-drying of foods*; F. Fisher Eds.; National academy of science-national research council.
8. Martino, M. N., and Zaritzky, N. E. (1988) Ice crystal size modifications during frozen beef storage. *J. Food Sci.* **53**, 1631-1637.
9. Min, S. G. (1994) Untersuchungen zur Rekristallisation von Eis in gefrorenen Lebensmitteln. Dissertation, Hohenheim University
10. Miyawaki, O., Abe, T., and Yano, T. (1992) Freezing and ice structure formed in protein gels. *Biosci. Biotechnol. Biochem.* **56**, 953-957.
11. Reid, D. S. (1990) Optimizing the quality of frozen foods. *Food Technol.* **44**, 78-82.
12. Tamon, H., Ishizaka, H., Yamamoto, T., and Suzuki, T. (2001) Freeze-drying for preparation of aerogel-like carbon. *Drying Technol.* **19**, 313-324.
13. Woinet, B., Andrieu, J., and Laurent, M. (1998a) Experimental and theoretical study of model food freezing. Part I. Heat transfer modeling. *J. Food Eng.* **35**, 381-393.
14. Woinet, B., Andrieu, J., Laurent, M., and Min, S. G. (1998b) Experimental and theoretical study of model food freezing. Part II: Characterization and modeling of the ice crystal size. *J. Food Eng.* **35**, 395-407.

(2008. 7. 2 접수/2008. 8. 4 수정/2008. 8. 8 채택)